

A Galerkin Layerwise Formulation for three-dimensional stress analysis in long sandwich plates

Isa Ahmadi *

*Advanced Materials and computational Mechanics Lab., Department of Mechanical Engineering,
University of Zanjan, 45371-38791, Zanjan, Iran*

(Received December 01, 2016, Revised April 12, 2017, Accepted May 03, 2017)

Abstract. A layerwise (LW) formulation based on the Galerkin method is presented to investigate the three-dimensional stress state in long sandwich plate which is subjected to tension force and pure bending moment. Based on the Galerkin method and the LW discretization approach, the equilibrium equations of elasticity for the long plate are written in the weak form and discretized through the thickness of the plate. The discretized equations are written in terms of displacement components of the numerical layers. The governing equations of the plate are solved analytically for the free edge boundary conditions. The distribution of stress state especially the 3D stress state in the vicinity of the edges of the sandwich plate which is subjected to tension and pure bending is studied. In order to increase the accuracy, the out of plane stresses are obtained by integrating the equilibrium equations of elasticity. The convergence and accuracy of the predictions are studied and various numerical results are presented for distribution of the in-plane and out of plane stresses in symmetric and un-symmetric sandwich plates.

Keywords: Galerkin Layerwise Formulation; long sandwich plate; 3D stress analysis; weak formulation

1. Introduction

The application of sandwich structures with composite faces is increasing in many industries. Due to excellent mechanical properties, sandwich structures with composite faces are used in light weight structures especially in civil engineering, automotive and aerospace industries. These mechanical properties mainly include excellent flexural stiffness and strength to mass ratio. Although sandwich structures have many advantages, delamination of core-face interface, especially near the free edges is one of the main problems in application of sandwich structure. Delamination occurs because of the out of plane normal and shear stresses which arise in core-face interface and interface of layers in vicinity of the edges which is called boundary-layer. Out of plane stresses usually increases due to mismatch between the material properties of face and core and geometric discontinuity near the free edge of the sandwich structures. Accurate determination of three-dimensional stress state in the boundary-layer regions of sandwich and laminated plates and shells is therefore crucial in order to correctly describe the structure behavior and to prevent their early failure. Generally, 3D exact elasticity solution must be used to obtain the 3D stress state accurately near the edges, but for general case this solution is not found yet and usually approximate and technical methods are used to predict the out-of plane stresses in sandwich and laminated plates. A brief literature survey of the previous research on the prediction of the 3D stress in

the sandwich and composite plates is given here.

Pipe and Pagano (1970) employed a finite-difference solution technique to obtain interlaminar stresses in composite laminates under uniform axial extension. Wang and Crossman (1977) examined the stress field of a finite-width, symmetrical laminate when subjected to a uniform temperature change. A finite-element formulation of equations governing layered anisotropic composite subjected to thermal and mechanical loadings provided by Reddy and Hsu (1980). They examined effects of shear deformation and anisotropy on thermal bending of layered composite plates.

Stein 1986 developed a 2D theory wherein in addition to the usual algebraic terms, the trigonometric through-the-thickness displacement terms are added to give more accurate results. Murthy and Chamis (1989) obtained interlaminar stresses in composite laminates under various loadings such as in-plane and out-of-plane sheary bending using a three-dimensional finite element method. Lu and Liu (1991) developed an Interlaminar Shear Stress Continuity Theory (ISSCT) to determine the interlaminar shear stress directly from the constitutive equations. Due to neglecting the deformation in the thickness direction, this theory could not calculate the interlaminar normal stress directly from the constitutive equations. Wu and Kuo (1992) used a local higher order lamination theory and predicted interlaminar stresses in composite laminates under cylindrical bending. Rohwer (1992) studied and compared various higher-order shear deformation theories for the bending analysis of composite plates and highlighted the advantages and disadvantages of the various theories.

Robbins and Reddy (1993) developed a layerwise finite element model of laminated composite plates and showed

*Corresponding author, Assistant Professor,
E-mail: i_ahmadi@znu.ac.ir

that their model is capable of computing interlaminar stresses and other localized effects with the same level of accuracy as a conventional three-dimensional finite element model. They analyzed bending of simply supported square laminated plates and free edge effects in symmetric angle-ply laminates subjected to axial displacements on the ends. Kim and Atluri (1994) examined interlaminar stresses near straight free edges of beam-type composite laminates under out of-plane sheary bending. They used an approximate method based on equilibrated stress representations and the use of the principle of minimum complementary energy and found that interlaminar stresses under the sheary bending might exhibit substantially different characteristics than under uniaxial loading or under pure bending. Yin 1994 used Lekhnitskii's stress functions in each layer and employed the variational principle of complimentary virtual work and presented an approximate analytical method to study the free-edge stresses due to thermal and mechanical loads. Basar and Ding (1995) utilized the theoretical fundamentals for a 2D layer-wise shell theory including transverse shear and transverse normal strains and analyzed interlaminar stresses in composites. Robbins and Reddy (1996) presented a displacement-based variable kinematic global-local finite element method. Their displacement field hierarchy contains both a conventional plate expansion (2-D) and a full layerwise (3-D) expansion.

Unlike the single layer theories, the LWTs assume separate displacement field expansions within each layer and thereby provide a more kinematically correct representation of the strain field in each discrete layer of the laminate and also allow accurate ply-level stresses to be determined. Lee and Chen (1996) employed a layerwise interlaminar shear stress continuity theory with layer reduction technique to predict interlaminar shear stresses. They considered no thickness stretching in their analysis and obtained only shear transverse stresses.

Shu and Soldatos (2000) determined stress distributions in angle-ply laminated plates subjected to the cylindrical bending with different sets of edge boundary conditions. In an effort to determine the interlaminar stresses, an iterative technique in conjunction with the extended Kantorovich method is presented by Cho and Kim (2000) for thermal and mechanical loads. Bařar *et al.* (2000) developed a multi-layer shell elements approach to analyze the interlaminar stresses in the composite laminates. Rohwer *et al.* (2001) investigated the transverse shear and normal stresses in composite laminates subjected to thermal loading by using the extended two-dimensional method and the first-order shear deformation plate theory (FSDT). Huang *et al.* (2002) used a partially hybrid stress element with interlaminar continuity and analyzed bending of composite laminated plates. Matsunaga (2002) obtained stress and displacement distributions of simply supported cross-ply laminated composite and sandwich plates subjected to lateral pressure using a global higher-order plate theory. Tahani and Nosier (2003) used Reddy's LWT to analyze interlaminar stresses in general symmetric and unsymmetric cross-ply laminates with finite dimensions subjected to uniform axial extension. Matsunaga (2004) compared 2-D single-layer and 3-D layerwise theories for computing out-

of-plane stresses of cross-ply laminated composite and sandwich plates subjected to thermal loadings. Hosseini Kordkheili and Naghdabadi (2005) introduced a finite element formulation for analysis of FG plates and shells. Zhu *et al.* (2007) studied the dynamic interlaminar stress in laminated plates in free vibration and thermal load based on thermo-elasto-dynamic differential equations.

Nosier and Bahrami (2007) used the layerwise theory and investigated the interlaminar stresses in Angle-ply composite laminates. Mittelstedt and Becker (2008) utilized Reddy's layerwise laminate plate theory to obtain the closed-form analysis of free-edge effects in layered plates of arbitrary non-orthotropic layups. The approach consists of the subdivision of the physical laminate layers into an arbitrary number of mathematical layers through the plate thickness. Jin (2008) used a finite element model based on the layerwise theory (LWT) and the Von-Karman type nonlinear strains are used to analyze damage in laminated composite beams. In the formulation, the Heaviside step function is employed to express the discontinuous interlaminar displacement field at the delaminated interfaces.

Kim *et al.* (2012) analyzed interlaminar stresses near free edges in composite laminates by considering interface modeling. This interface modeling provided not only non-singular stresses but also concentrated finite interlaminar stresses using the principle of complementary virtual work. Cetkovic and Vuksanovic (2011) used the displacement layerwise method and studied the large deflection of the composite plate using small strain large displacement relation. Xiaohui *et al.* (2011) proposed a higher-order zig-zag theory for laminated composite and sandwich structures. Their proposed theory satisfies the interlaminar continuity conditions and free surface conditions of transverse shear stresses. They compared the transverse shear stress of their theory by the results of exact solution. Yasin and Kapuria (2013) extended a previously developed four-node quadrilateral element for laminated plates based on an efficient layerwise theory which is called the zig-zag theory (ZIGT) to laminated shallow shells. A three-dimensional multi-term extended Kantorovich method is utilized by Tahani and Andakhsideh (2012) to analyze the inter-laminar stresses, which are resulted from bending of thick rectangular laminated plates. Their obtained results were compared with those stated in the literature, which showed an excellent agreement.

Huang and Kim (2014) proposed a stress function-based approach and the principle of complementary virtual work to analyze the free-edge interlaminar stresses of piezobonded symmetric laminates. The proposed method satisfies the traction free boundary conditions, as well as surface free conditions. Hamidi *et al.* (2015) presented a 5-parameter sinusoidal plate theory for the thermomechanical bending analysis of functionally graded sandwich plates. Murugesan and Rajamohan (2015) studied the combined effects of thermal and mechanical loadings on the interlaminar shear stresses of composite laminated beams using the commercially available Finite element software package.

Ahmadi (2016) studied the interlaminar stresses in the cross-ply thick composite panel which is subjected to pure

extension force using the layerwise formulation employing the principle of minimum total potential energy. Kim *et al.* (2016) established systematically relationship between two independent displacement and stress fields through the mixed variational theorem (MVT) and studied the interlaminar stresses in composite and sandwich beam using a conventional higher order shear deformation theory (HSDT). Ahmadi and Najafi (2016) studied the three-dimensional stresses in thin laminated composite cylindrical shell subjected to the rotational body force using the principle of minimum total potential energy.

In this study a layerwise formulation based on the Galerkin weak formulation method is developed to study the 3D stress state in the sandwich plate which is subjected to axial tension and bending moment. For this purpose, the displacement field for a sandwich plate which is subjected to bending, twisting and tension is discretized through the plate thickness. The governing equations of the plate in the discrete form are obtained based on the weak formulation employing the Galerkin method and layerwise discretization approach. The discretized governing equations include a set of ordinary differential equations which are named the local equilibrium equations associated to numerical layers. The local equilibrium equations and global equilibrium equations are solved analytically for a plate with free edge conditions. A 3D finite element modeling is used for verification of the results of the present study. In the numerical results the out of plane and in-plane stresses in sandwich plate which is subjected to tension, bending and torsion are investigated. The out of plane stresses satisfy the traction-free conditions at the top and bottom surfaces of the plate.

2. Modelling

Consider a long sandwich plate with laminated composite faces with orthotropic layers. The length of the plate is $2L$, the thickness is h and the width is $2b$. The coordinate system xyz is assigned to the plate at its center as shown in Fig. 1. It is supposed that the plate is long and subjected to pure bending moment M_x and extension force F_x at its ends at $x = L$ and $x = -L$.

For the long plate which is subjected to this kind of loading conditions, it can be supposed that far from the loading edges at $x = \pm L$, the strain and stress field is uniform in the length of the plate and do not depend on the x -coordinate. For the plate for which the stresses (and strains) are uniformly distributed in the x direction, the equilibrium equations can be written as

$$\begin{aligned}\sigma_{xy,y} + \sigma_{xz,z} &= 0 \\ \sigma_{y,y} + \sigma_{yz,z} &= 0 \\ \sigma_{yz,y} + \sigma_{z,z} &= 0\end{aligned}\quad (1)$$

in which the derivations with respect to the x coordinate are ignored. In this study a displacement based layerwise theory is used to discretize the governing equations of the plate.

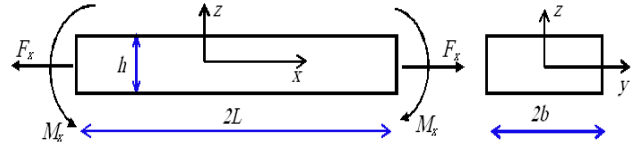


Fig. 1 Sandwich plate subjected to pure bending moment and extension force

2.1 Layerwise discretization approach

In the equivalent single layer (ESL) theories such as the classical and first order shear deformation theories, it is assumed that the laminated or sandwich plates and shells deform as a single layer structure. These theories consider a kind of lumping in the deformation field of the laminate in the thickness. The assumed deformation field in the classical theory and first order shear deformation theory (FSDT) leads to ignoring or considering uniform out of plane strains through the thickness of the laminate. Although these theories can predict the overall response of the plates and shells and the in-plane stresses, they can not accurately evaluate (characterize) the local phenomena in the laminates such as the out of plane stresses and boundary layer phenomena.

Unlike the equivalent single layer (ESL) theories, the layerwise theories (LWT) are developed in order to give more flexibility to the plies of the laminate to deform approximately the same as the deformation of an elastic material. So, the displacement based layer-wise theories can predict the displacement field in the laminate more accurately and are able to predict the out of plane stresses through the thickness of the laminates and model the local phenomena such as the 3D stress state in the vicinity of the edges.

In the LWT which is used in this study, each actual layer in the laminate is subdivided into arbitrary number of layers through the plate thickness which are called numerical layers. For a laminate that is subdivided into N numerical layers, including the bottom and top surfaces of the laminate, $N + 1$ numerical surfaces can be considered in the laminate which are numbered from bottom to the top surface of the laminate and the k^{th} numerical surface are located at $z = z_k$. In the displacement based layerwise theory the value of displacement inside the numerical layers are interpolated from its values on the numerical surfaces. For example the value of unknown displacement such as $u(x, y, z)$ can be discretized in the z direction as

$$u(x, y, z) = \sum_{k=1}^{N+1} \Phi_k(z) U_k(x, y) \quad (2)$$

in which $\Phi_k(z)$ is known as linear Lagrangian interpolation function and $U_k(x, y)$ is the value of the displacement $u(x, y, z)$ on the k^{th} numerical surface. Eq. (2) in the matrix form can be written as

$$u(x, y, z) = \{\Phi(z)\} \{U(x, y)\} \quad (3)$$

$\{\Phi(z)\}$ is the matrix of interpolation function and $\{U(x, y)\}$ is the matrix which include displacement of numerical surface and are defined as

$$\begin{aligned}\{\Phi\} &= \{\Phi_1(z), \Phi_2(z), \dots, \Phi_{N+1}(z)\} \\ \{U\} &= \{U_1(x, y), U_2(x, y), \dots, U_{N+1}(x, y)\}^T\end{aligned}\quad (4)$$

The linear Lagrangian interpolation function in the thickness of the plate, $\Phi_k(z)$, can be represented as

$$\Phi_k(z) = \begin{cases} \frac{(z - z_{k-1})}{t_{k-1}}, & z \leq z_{k-1} \\ \frac{(z_{k+1} - z)}{t_k}, & z_{k-1} \leq z \leq z_k \\ 0, & z \leq z_{k-1} \text{ or } z \geq z_{k+1} \end{cases} \quad (5)$$

where t_k is the thickness of the k^{th} numerical layer and z_k is the thickness coordinate of the k^{th} numerical surface.

2.2 Galerkin formulation

The weak formulation based on the Galerkin method is used to obtain the governing equations of the plate in the layerwise discretization approach. In order to obtain the Galerkin formulation, the equilibrium equations in Eq. (1) are multiplied by the Lagrangian interpolation functions $\{\Phi(z)\}^T$ and are integrated in the thickness direction to obtain the following equations.

$$\begin{aligned}\int_{-h/2}^{h/2} (\{\Phi\}^T \sigma_{xy})_{,y} dz - \int_{-h/2}^{h/2} \{\Phi\}'^T \sigma_{xz} dz + (\{\Phi\}^T \sigma_{xz}) \Big|_{-h/2}^{h/2} &= 0 \\ \int_{-h/2}^{h/2} (\{\Phi\}^T \sigma_y)_{,y} dz - \int_{-h/2}^{h/2} \{\Phi\}'^T \sigma_{yz} dz + (\{\Phi\}^T \sigma_{yz}) \Big|_{-h/2}^{h/2} &= 0 \quad (6) \\ \int_{-h/2}^{h/2} (\{\Phi\}^T \sigma_{yz})_{,y} dz - \int_{-h/2}^{h/2} \{\Phi\}'^T \sigma_z dz + (\{\Phi\}^T \sigma_z) \Big|_{-h/2}^{h/2} &= 0\end{aligned}$$

where the integration by part is applied in the above equation. The prime on $\{\Phi(z)\}$ i.e., $\{\Phi(z)\}'$ represents ordinary differentiation with respect to z . According to the appeared integrals in Eq. (6), the stress resultants are defined as

$$\begin{aligned}(\{M_y\}, \{M_{xy}\}, \{R_y\}) &= \int_{-h/2}^{h/2} (\{\Phi\}^T \sigma_y, \{\Phi\}'^T \sigma_{xy}, \{\Phi\}'^T \sigma_{yz}) dz \\ (\{Q_x\}, \{Q_y\}, \{N_z\}) &= \int_{-h/2}^{h/2} (\{\Phi\}'^T \sigma_{xz}, \{\Phi\}'^T \sigma_{yz}, \{\Phi\}'^T \sigma_z) dz\end{aligned}\quad (7)$$

in which for example $\{M_y\}$ and other stress resultants which are defined in Eq. (7) are column matrixes with $(N+1)$ component. The third terms in Eq. (6) impose the applied loads on the top and bottom surfaces of the plate to the formulation. In this study the top and bottom surfaces of the plate are traction free and so the third terms in Eq. (6) vanish. By substituting the stress resultants from Eq. (7) into Eq. (6) and assuming the traction free surfaces, the governing equations of the plate in the weak form are obtained as

$$\begin{aligned}\{M_{xy}\}_{,y} - \{Q_x\} &= \{0\} \\ \{M_y\}_{,y} - \{Q_y\} &= \{0\} \\ \{R_y\}_{,y} - \{N_x\} &= \{0\}\end{aligned}\quad (8)$$

It is clear that Eq. (8) includes $3(N+1)$ ordinary differential equations which are written in the matrix form. On the other hand, the weak form of the free edge boundary conditions for the plate at $y = \pm b$ can be obtained by multiplying the traction free conditions i.e., $\sigma_{xy} = 0$, $\sigma_y = 0$ and $\sigma_{yz} = 0$, by $\{\Phi\}^T$ and integrating over the thickness of the plate as

$$\begin{aligned}\{M_{xy}\} &= \{0\} \\ \{M_y\} &= \{0\} \text{ at } y = \pm b \\ \{R_y\} &= \{0\}\end{aligned}\quad (9)$$

Imposing the boundary conditions in $y = \pm b$ includes satisfaction of $3(N+1)$ equations.

2.3 Navier equations

The displacements of a material point in the length, width and thickness direction of the plate are shown by $u_1(x, y, z)$, $u_2(x, y, z)$ and $u_3(x, y, z)$, respectively. For the long plate, the strain field does not depend on the length coordinate x , the reduced displacement field can be obtained by integrating the strain-displacement relation of the plate and considering in the mind that the strain components do not depend on the x -coordinate. By integrating the strain components and ignoring the rigid body motion and rigid body rotation from the displacement field, the general form of the displacement field of the plate can be obtained as (Lekhnitskii 1981)

$$\begin{aligned}u_1(x, y, z) &= C_5 xz + C_6 x + u(y, z) \\ u_2(x, y, z) &= -C_3 xz + v(y, z) \\ u_3(x, y, z) &= -\frac{1}{2} C_5 x^2 + C_3 xz + w(y, z)\end{aligned}\quad (10)$$

in which $u(y, z)$, $v(y, z)$ and $w(y, z)$ are unknown displacement functions of y and z co-ordinate and C_5 , C_6 and C_3 are constants. From the displacement field in Eq. (10) it can be concluded that C_6 is the constant normal strain of the mid plane ($z = 0$) in the x direction, $C_5 x$ is the rotation angle of the yz sections of the plate about the y axis, and $C_3 x$ is the rotation angle of the yz sections of the plate about the x axis in the negative direction. It can be concluded that C_3 , C_5 and C_6 are the global response of the plate which show twisting, bending and extension of plane and $u(y, z)$, $v(y, z)$ and $w(y, z)$ are displacements which indicate the local response of the plate to the external loading. To employ the LWT, the value of the unknown displacement $u(y, z)$, $v(y, z)$ and $w(y, z)$ (see Eq. (10)) on the i^{th} numerical surface are shown by $U_i(y)$, $V_i(y)$, and $W_i(y)$ which are unknown functions of y -coordinate and must be obtained in problem solution. The displacement function $u(y, z)$, $v(y, z)$ and $w(y, z)$ can be interpolated within numerical layers $U_i(y)$, $V_i(y)$, and $W_i(y)$ and the interpolation functions. According to the

displacement field in Eq. (10), and LW discretization approach Eq. (3), the displacement field of the plate in the LWT can be written in the discretized form as

$$\begin{aligned} u_1 &= \{\Phi\} \{U\} + C_5 xz + C_6 x \\ u_2 &= \{\Phi\} \{V\} - C_3 xz \\ u_3 &= \{\Phi\} \{W\} - \frac{1}{2} C_5 x^2 + C_3 xz \end{aligned} \quad (11)$$

where $\{\Phi(z)\}$ is the matrix of interpolation functions in the z direction and defined in Eq. (4), and $\{U(y)\}$, $\{V(y)\}$ and $\{W(y)\}$ are column $(N+1)$ matrix and are defined as

$$\begin{aligned} \{U\} &= \{U_1(y), U_2(y), \dots, U_{N+1}(y)\}^T \\ \{V\} &= \{V_1(y), V_2(y), \dots, V_{N+1}(y)\}^T \\ \{W\} &= \{W_1(y), W_2(y), \dots, W_{N+1}(y)\}^T \end{aligned} \quad (12)$$

By substituting the displacement field Eq. (12) into the strain-displacement relations, the strain components in the plate can be obtained as

$$\begin{aligned} \varepsilon_x &= C_6 + C_5 z, & \varepsilon_{xy} &= \{\Phi\} \{U\}' - C_3 z, \\ \varepsilon_y &= \{\Phi\} \{V\}', & \varepsilon_{xz} &= \{\Phi\}' \{U\} + C_3 y, \\ \varepsilon_z &= \{\Phi\}' \{W\}, & \varepsilon_{yz} &= \{\Phi\}' \{V\} + \{\Phi\} \{W\}' \end{aligned} \quad (13)$$

in which the prime on $\{U\}$, $\{V\}$ and $\{W\}$ represents ordinary differentiation with respect to y and the prime on $\{\Phi\}$ represents ordinary differentiation with respect to z . Eq. (7) shows the strain field in the plate which is discretized in z direction.

The stresses in the k^{th} orthotropic numerical layer in the plate can be obtained by using the constitutive law of the stress-strain relation as

$$\{\sigma\}^{(k)} = [\bar{C}]^{(k)} \{\varepsilon\}^{(k)} \quad (14)$$

in which $[\bar{C}]^{(k)}$ is the stiffness matrix of orthotropic layers and are shown in the Appendix A in Eq. (A1) and $\{\sigma\}$ and $\{\varepsilon\}$ are defined as

$$\begin{aligned} \{\sigma\} &= \{\sigma_x, \sigma_y, \sigma_z, \sigma_{yz}, \sigma_{xz}, \sigma_{xy}\}^T \\ \{\varepsilon\} &= \{\varepsilon_x, \varepsilon_y, \varepsilon_z, \varepsilon_{yz}, \varepsilon_{xz}, \varepsilon_{xy}\}^T \end{aligned} \quad (15)$$

The stresses and strains are substituted from the stress-strain relation Eq. (14) and strains from Eq. (7) into Eq. (10) and the subsequent results are substituted into Eq. (11) and the $3(N+1)$ local equilibrium equations of the plate Eq. (11) are obtained in terms of the displacement components as

$$\begin{aligned} &[D_{66}]\{U\}'' + [D_{26}]\{V\}'' + ([B_{36}] - [B_{45}]^T)\{W\}' \\ &- [A_{55}]\{U\} - [A_{45}]\{V\} = \{A_{55}\}C_3 y \\ &[D_{26}]\{U\}'' + [D_{22}]\{V\}'' + ([B_{23}] - [B_{44}]^T)\{W\}' \\ &- [A_{45}]\{U\} - [A_{44}]\{V\} = \{A_{45}\}C_3 y \\ &[D_{44}]\{W\}'' + ([B_{45}] - [B_{36}]^T)\{U\}' + ([B_{44}] - [B_{23}]^T)\{V\}' \\ &- [A_{33}]\{W\} = -(\{\tilde{A}_{36}\} + \{B_{45}\})C_3 + \{\tilde{A}_{13}\}C_5 + \{A_{13}\}C_6 \end{aligned} \quad (16)$$

in which the coefficient matrices $[A_{pq}]$, $[B_{pq}]$, $[D_{pq}]$ are $(N+1) \times (N+1)$ square matrices and $\{A_{pq}\}$, $\{B_{pq}\}$ and $\{\tilde{B}_{pq}\}$ are $(N+1) \times 1$ column matrix and are so-called the rigidity matrices in the LWT and are defined as

$$\begin{aligned} ([A_{pq}], [B_{pq}]) &= \int_{-h/2}^{h/2} (\bar{C}_{pq} \{\Phi\}'^T \{\Phi\}', \bar{C}_{pq} \{\Phi\}^T \{\Phi\}') dz \\ [D_{pq}] &= \int_{-h/2}^{h/2} \bar{C}_{pq} \{\Phi\}^T \{\Phi\} dz \\ (\{A_{pq}\}, \{B_{pq}\}) &= \int_{-h/2}^{h/2} (\bar{C}_{pq} \{\Phi\}'^T, \bar{C}_{pq} \{\Phi\}^T) dz \\ (\{\tilde{A}_{pq}\}, \{\tilde{B}_{pq}\}) &= \int_{-h/2}^{h/2} (\bar{C}_{pq} z \{\Phi\}'^T, \bar{C}_{pq} z \{\Phi\}^T) dz \end{aligned} \quad (17)$$

The terms of the rigidity matrices are calculated and can be seen in Appendix A.

2.4 Loading conditions

It is obvious that the global equilibrium equations of the plate which is subjected to global extension force F_x and bending moment M_x at $x = \pm L$ can be written as

$$\begin{aligned} \int_{-b}^b \int_{-h/2}^{h/2} \sigma_x dz dy &= F_x \\ \int_{-b}^b \int_{-h/2}^{h/2} \sigma_x z dz dy &= M_x \\ \int_{-b}^b \int_{-h/2}^{h/2} (\sigma_{xz} y - \sigma_{xy} z) dz dy &= 0 \end{aligned} \quad (18)$$

The global equilibrium equations of the plate Eq. (18) can be written in terms of the displacement as

$$\begin{aligned} &2b\bar{A}_{11}C_6 + 2b\bar{A}_{11}C_5 - 2b\bar{A}_{16}C_3 + \\ &\int_{-h/2}^{h/2} (\{B_{16}\}^T \{U\}' + \{B_{12}\}^T \{V\}' + \{A_{13}\}^T \{W\}) dy = F_x \\ &2b\bar{A}_{11}C_6 + 2b\bar{A}_{11}C_5 - 2b\bar{A}_{16}C_3 + \\ &\int_{-h/2}^{h/2} (\{\tilde{B}_{16}\}^T \{U\}' + \{\tilde{B}_{12}\}^T \{V\}' + \{\tilde{A}_{13}\}^T \{W\}) dy = M_x \\ &-2b\bar{A}_{16}C_6 - 2b\bar{A}_{16}C_5 + (2b\bar{A}_{66} + \frac{2}{3}b^3\bar{A}_{55})C_3 + \\ &\int_{-h/2}^{h/2} (-\{\tilde{B}_{66}\}^T \{U\}' - \{\tilde{B}_{26}\}^T \{V\}' - \{\tilde{A}_{36}\}^T \{W\}) dy + \\ &\int_{-h/2}^{h/2} (\{A_{55}\}^T \{U\} + \{A_{45}\}^T \{V\} + \{B_{45}\}^T \{W\}') dy = 0 \end{aligned} \quad (19)$$

where in Eq. (19), the global rigidities of the plate are defined as

$$(\bar{A}_{pq}, \bar{A}_{pq}, \bar{A}_{pq}) = \sum_{i=1}^N \int_{z_i}^z \bar{C}_{pq}^{(i)} (1, z, z^2) dz \quad (20)$$

2.5 Solution of equations

The governing equations of the plate include $3(N+1)$ differential equations which are seen in Eq. (16) and 3 global equilibrium equation which is presented in Eq. (19). To solve them, the set of differential equations in Eq. (16) is written in the matrix form. To this aim the state matrix $\{X\}$

which is a column matrix is defined as

$$\{X\} = \{ \{U\}^T, \{U'\}^T, \{V\}^T, \{V'\}^T, \{W\}^T, \{W'\}^T \}^T \quad (21)$$

By using the matrix $\{X\}$, the local equilibrium equations of plate in Eq. (16) can be written in the matrix form as

$$\{X\}' = [C]\{X\} + \{F_{31}\}C_3 + \{F_{32}\}C_3y + \{F_5\}C_5 + \{F_6\}C_6 \quad (22)$$

where the coefficient matrices which are seen in Eq. (21) are defined in Appendix B. Using the eigen-value and eigen-vectors of $[C]$, the solution of Eq. (22) is obtained as

$$\begin{aligned} \{X\} &= [U] \exp([A]y) \{K\} - \\ [C]^{-1} (\{F_{31}\}C_3 + \{F_{32}\}C_3y + \{F_5\}C_5 + \{F_6\}C_6) \end{aligned} \quad (23)$$

in which $[U]$ is the matrix of eigen-vectors and $[A]$ is the matrix of eigen-values of $[C]$ which are defines as

$$\begin{aligned} [C][U] &= [U][A] \\ [A] &= \text{diag}(\lambda_1, \lambda_2, \dots, \lambda_{N+1}) \end{aligned} \quad (24)$$

where $\lambda_1, \lambda_2, \dots$ and λ_{N+1} are the eigen-values of $[C]$ and $\{F_3\}$ is defined as

$$\{F_3\} = \{F_{31}\} + [A]^{-1} \{F_{32}\} \quad (25)$$

and $\{K\}$ is a column matrix contains $6(N+1)$ unknown constants of integration. The unknowns must be obtained by imposing the boundary conditions of the plate at the edges $y = \pm b$ and considering the global loading conditions of the plate in Eq. (19).

2.6 Imposing boundary and loading conditions

As seen in Eq. (9), the free edge conditions for the plate include imposing $\{M_y\} = \{0\}$, $\{R_y\} = \{0\}$ and $\{M_{xy}\} = \{0\}$ at $y = \pm b$. The boundary conditions can be written in terms of the displacements as

$$\begin{aligned} \{M_y\} &= [D_{26}]\{U'\} + [D_{22}]\{V'\} + [B_{23}]\{W\} \\ &+ \{B_{12}\}C_6 + \{\tilde{B}_{12}\}C_5 - \{\tilde{B}_{26}\}C_3 = \{0\} \\ \{R_y\} &= [B_{45}]\{U\} + [B_{44}]\{V\} + [D_{44}]\{W'\} \\ &+ \{B_{45}\}C_3y = \{0\} \\ \{M_{xy}\} &= [D_{66}]\{U'\} + [D_{26}]\{V'\} + [B_{36}]\{W\} \\ &+ \{B_{16}\}C_6 + \{\tilde{B}_{16}\}C_5 - \{\tilde{B}_{66}\}C_3 = \{0\} \end{aligned} \quad (26)$$

It is obvious that imposing Eq. (26) both at $y = b$ and $y = -b$, includes satisfaction of $6(N+1)$ equations. Considering the state matrix $\{X\}$ which is defined in Eq. (21), the boundary conditions Eq. (26) can be written as

$$\begin{aligned} [P_1]\{X(\pm b)\} + \{B_{12}\}C_6 + \{\tilde{B}_{12}\}C_5 - \{\tilde{B}_{26}\}C_3 &= \{0\} \\ [P_2]\{X(\pm b)\} + \{B_{45}\}(\pm b)C_3 &= \{0\} \\ [P_3]\{X(\pm b)\} + \{B_{16}\}C_6 + \{\tilde{B}_{16}\}C_5 - \{\tilde{B}_{66}\}C_3 &= \{0\} \end{aligned} \quad (27)$$

in which $[P_1]$, $[P_2]$ and $[P_3]$ are defined as

$$\begin{aligned} [P_1] &= \{[0], [D_{26}], [0], [D_{22}], [B_{23}], [0]\} \\ [P_2] &= \{[B_{45}], [0], [B_{44}], [0], [0], [D_{44}]\} \\ [P_3] &= \{[0], [D_{66}], [0], [D_{26}], [B_{36}], [0]\} \end{aligned} \quad (28)$$

By employing $\{X\}$, the global equilibrium equations for extension and bending of the plate can be written as follow.

$$\begin{aligned} \int_{-h/2}^{h/2} \{M_1\} \{X\} dy + 2b\bar{A}_{11}C_6 + 2b\bar{A}_{11}C_5 - 2b\bar{A}_{16}C_3 &= F_x \\ \int_{-h/2}^{h/2} \{M_2\} \{X\} dy + 2b\bar{A}_{11}C_6 + 2b\bar{A}_{11}C_5 - 2b\bar{A}_{16}C_3 &= M_x \end{aligned} \quad (29)$$

in which according to Eqs. (19) and (21), $\{M_1\}$, $\{M_2\}$ are defined as

$$\begin{aligned} \{M_1\} &= \{\{0\}^T, \{B_{16}\}^T, \{0\}^T, \{B_{12}\}^T, \{A_{13}\}^T, \{0\}^T\}^T \\ \{M_2\} &= \{\{0\}^T, \{\tilde{B}_{16}\}^T, \{0\}^T, \{\tilde{B}_{12}\}^T, \{\tilde{A}_{13}\}^T, \{0\}^T\}^T \end{aligned} \quad (30)$$

The displacement field which is obtained in Eq. (23) has unknown constants include $\{K\}$ and the unknown displacement constants C_3 , C_5 and C_6 . These unknown constants in the displacement field depend on boundary and loading conditions and must be obtained by imposing the loading and boundary conditions of the plate. For this purpose, the displacement field in Eq. (23) is substituted into boundary and loading conditions in Eqs. (27) and (29) and a set of algebraic equations is obtained. The set of algebraic equations is solved simultaneously to obtain the unknown constants $\{K\}$ and unknown displacement constants C_3 to C_6 . By obtaining the unknown constants, the stresses are obtained by the procedure which is explained in the next section.

2.7 Out of plane stresses

The stress components can be obtained by the stress-strain relations. The in-plane stresses are obtained by stress-strain relation, but in an alternative method, the out of plane stresses can be obtained by integrating the equilibrium equations of elasticity. The out of plane stresses which are predicted by integrating the equilibrium equations are continuous at the thickness of the plate and are more accurate. In integrating method, the in-plane stresses are substituted from the stress-strain relations into the equilibrium equations and the out of plane stresses are obtained by integrating the equations in z direction. For instance σ_{xz} at the n^{th} numerical surface ($z = z_n$) can be obtained as

$$\begin{aligned} \sigma_{xz}(z = z_n) &= -\int_{z_1}^{z_n} \frac{\partial \sigma_{xy}}{\partial y} dz \\ &- \int_{z_1}^{z_n} (\bar{C}_{26}\Phi_k V_k'' + \bar{C}_{36}\Phi_k' W_k' + \bar{C}_{66}\Phi_k U_k'') dz = \\ &= -\sum_{k=1}^n (\bar{B}_{26}^k V_k'' + \bar{A}_{36}^k W_k' + \bar{B}_{66}^k U_k'') \end{aligned} \quad (31)$$

where

$$(\bar{A}_{pq}^k, \bar{B}_{pq}^k) = \int_{z_1}^{z_n} (\bar{C}_{pq} \Phi_k', \bar{C}_{pq} \Phi_k) dz \quad k \leq n \quad (32)$$

In this study, the interlaminar stresses in the plate are obtained by the stress-strain relation and by integrating the equilibrium equations and the obtained results are compared.

3. Numerical results and discussions

The 3D stress state in sandwich plate which is subjected to tension, bending and twisting loading is studied. The faces of sandwich plate are made of laminated composite and can have arbitrary layer stacking and the core is made of foam. The face thickness is h_f , the core thickness is h_c , and the total thickness of the sandwich plate is $h = h_c + 2h_f$. The mechanical properties of the lamina and foam are tabulated in Table 1. The subscript c refers to core material.

3.1 Verification of the results

In order to verify the LW formulation and the accuracy of the solution which is presented in this study, the prediction of the present method is compared with the predictions of the FE modeling with Ansys. To this aim, a symmetric $[0^\circ/90^\circ/\text{core}/90^\circ/0^\circ]$ sandwich plate which is subjected to extension force F_x is modeled in the FE code Ansys using solid46 element. The sequence of the layers is written in the bracket from the bottom to the top of the plate, respectively. In order to obtain accurate results for out of plane stresses in the finite element modeling, the thickness and width of the plate are divided into 60 elements and 200 elements, respectively, and the length of the plate is divided into 8 elements. This FE model contains about 110000 nodes, and each node has 3 DOF, and the FE

model totally has about 330000 DOF. The same problem is solved using the presented LW formulation, in which the thickness of the plate is divided into 60 numerical layers. Each numerical surface has 3 DOF, so totally $3 \times (61) = 183$ DOF are used in the LW method. The predictions of the LWT and FE solutions are compared in Figs. 2 to 5 in order to verify the accuracy of the method. Computationally, the FE modeling is very expensive than the presented LW solution.

The distribution of the interlaminar normal stress σ_z and shear stress σ_{yz} along the width of the plate at $z = 0.5h_c$ (core-face interface) and at $z = 0.5(h_c + h_f)$ (90/0 interface) is presented in Figs. 2 and 3. The prediction of the LWT by constitutive law, by integration method, and the prediction of FEM are depicted in Figs. 2 and 3. For the plate which is subjected to axial extension force F_x , the dimensionless stress is defined as the ratio of the stress to the average axial stress as $\sigma^* = 2bh^2\sigma/F_x$. Both the constitutive law and integration of equilibrium equations are used to predict the out of plane stresses in the LW solution, and the predicted results of both methods are presented in Figs. 2 and 3. A look at this figure makes it clear that there is very good agreement between the predictions of FEM and LWT, except at the vicinity of the edge.

Exactly at the free edge, σ_z which is predicted by the

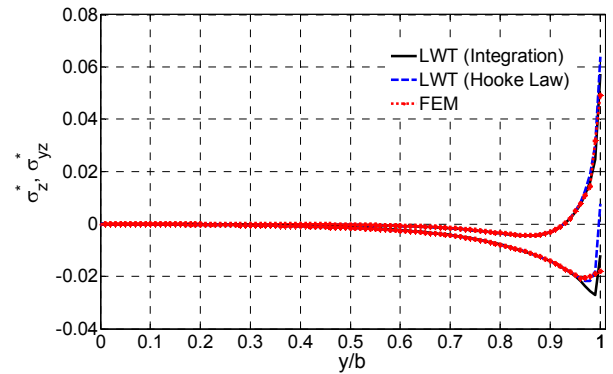


Fig. 3 Distribution of the out of plane stresses σ_z and σ_{yz} along $z = (h_c + h_f)/2$ of the plate ($[0^\circ/90^\circ/\text{core}/90^\circ/0^\circ]$, $h_f = 0.3h$, $h_c = 0.4h$, $b = 1.5h$)

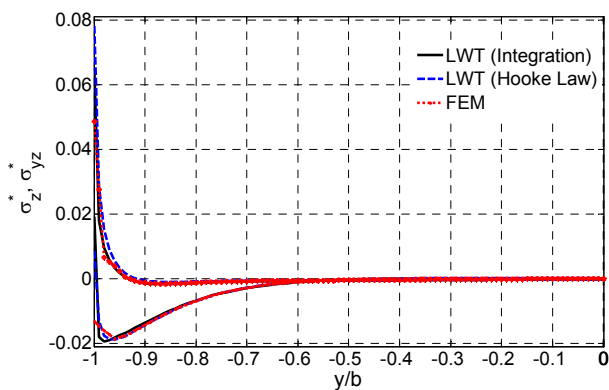


Fig. 2 Distribution of the out of plane stress σ_z and σ_{yz} along $z = h_c/2$ of the plate ($[0^\circ/90^\circ/\text{core}/90^\circ/0^\circ]$, $h_f = 0.3h$, $h_c = 0.4h$, $b = 1.5h$)

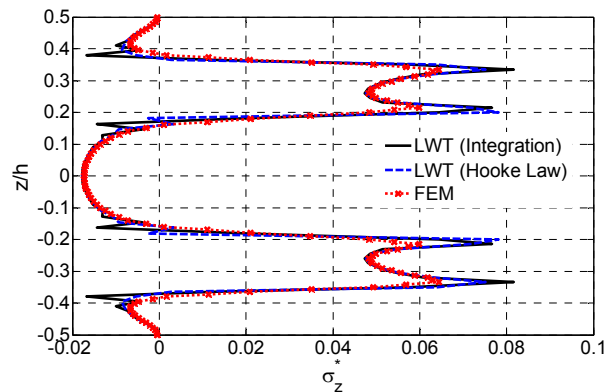


Fig. 4 Distribution of the out of plane stress σ_z through the thickness of the plate at edge $y = b$, ($[0^\circ/90^\circ/\text{core}/90^\circ/0^\circ]$, $h_f = 0.3h$, $h_c = 0.4h$, $b = 1.5h$)

Table 1 Elastic properties of Carbon/Epoxy lamina and foam (core) (Barbero 2013)

E_1 (GPa)	$E_2 = E_3$ (GPa)	$G_{12} = G_{13}$ (GPa)	G_{23} (GPa)	$\nu_{12} = \nu_{13}$	ν_{23}	E_c (GPa)	ν_c
138	8.5	4.5	3.2	0.29	0.36	3	0.4

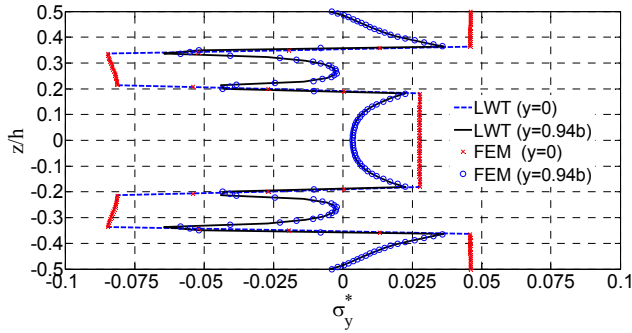


Fig. 5 Distribution of the in-plane normal stress σ_y through the thickness of the plate at $y = 0$ and $y = 0.94b$, $[0^\circ/90^\circ/\text{core}/90^\circ/0^\circ]$, $h_f = 0.3h$, $h_c = 0.4h$, $b = 1.5h$

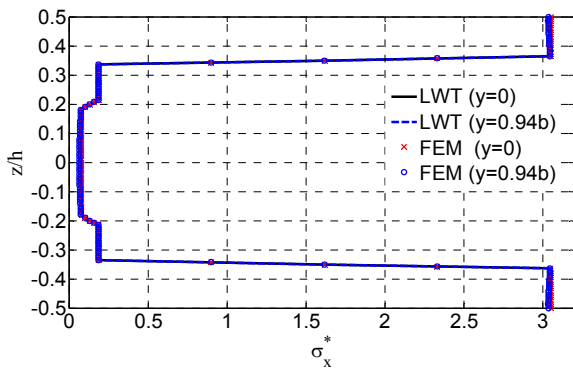


Fig. 6 Distribution of the in-plane normal stress σ_x through the thickness of the plate at $y = 0$ and $y = 0.94b$, $[0^\circ/90^\circ/\text{core}/90^\circ/0^\circ]$, $h_f = 0.3h$, $h_c = 0.4h$, $b = 1.5h$

LWT using the integration method is between the prediction of FEM and prediction of LWT using Hooke's law. It is seen that there is a difference between the LWT and FEM in prediction of shear stress σ_{yz} at the vicinity of edge.

In order to study more on prediction of the LWT and FEM, the distribution of the interlaminar normal stress σ_z

through the thickness of the plate at free edge ($y = b$) is presented in Fig. 4. This figure compares the predictions of the LWT (using Hooke's law and using integration method) and the predictions of the FEM. At the free edge, σ_z is increased sharply around the interfaces. From Figs. 2 to 4, it can be concluded that the prediction of LWT and FEM for out of plane stresses is in very good agreement except in the vicinity of the free edge near the interfaces. Exactly at the free edge, a difference is seen between the predictions of the LWT and FEM. The prediction of LWT for σ_z in the edge is bigger than the prediction of FEM. It must be noted that in the LWT the governing equations are discretized only in the thickness direction by Lagrangian interpolation functions and the equations are not discretized in y direction and the obtained set of ordinary differential equation is analytically solved. So it seems that the predictions of LWT for out of plane stresses are more accurate than the predictions of FEM.

To compare the predictions of FEM and LWT for in-plane stresses, the distribution of in-plane normal stress σ_y and σ_x through the thickness of the plate at $y = 0$ and $y = 0.94b$ in the $[0^\circ/90^\circ/\text{core}/90^\circ/0^\circ]$ sandwich plate which is subjected to extension load is shown in Figs. 5 and 6, respectively. There is very good agreement between the prediction of the FEM and LWT in prediction of the in-plane stresses. Considering Figs. 2 to 6, it is concluded that prediction of LWT is in good agreement with the prediction of the FEM, except in prediction of out of plane stresses near the free edge.

3.2 Convergence study

The convergence of the predictions of LWT with increasing the number of numerical layers is studied in Table 2.

Some researchers reported singularity of the out-of plane stresses in the free edge of plates and shells at the interfaces of physical layers with different elastic properties. The convergence of stresses with increasing the number of numerical layers in the $[30^\circ/-30^\circ/\text{core}/-30^\circ/30^\circ]$ sandwich plate ($h_c = 0.4h$, $h_f = 2 \times 0.15h$, $b = 1.5h$) which is subjected to bending moment M is studied in Table 2. The

Table 2 Convergence of the predictions of LWT, $[30^\circ/-30^\circ/\text{core}/-30^\circ/30^\circ]$ sandwich plate, ($h_c = 0.4h$, $h_f = 2 \times 0.15h$, $b = 1.5h$)

P	σ_z^* $z = h_c/2, y = b$	σ_z^* $z = (h_c + h_f)/2, y = b$	σ_{xz}^* $z = h_c/2, y = b$	σ_{xz}^* $z = (h_c + h_f)/2, y = b$	σ_{xz}^* $z = 0, y = b$	σ_x^* $z = h/2, y = 0$	σ_y^* $z = 0, y = 0$
1	-0.0543	-0.2064	0.2854	-1.0838	0.3566	5.1550	0.0704
2	0.0304	-0.2931	0.3769	-1.5490	0.2702	5.2093	0.0760
3	0.0479	-0.3797	0.3745	-1.8350	0.2873	5.2216	0.0779
4	-0.0276	-0.4406	0.3980	-2.0577	0.2802	5.2266	0.0789
5	-0.0429	-0.4885	0.4062	-2.2296	0.2824	5.2291	0.0795
6	-0.0439	-0.5272	0.4165	-2.3717	0.2818	5.2306	0.0798
7	-0.0484	-0.5597	0.4240	-2.4922	0.2821	5.2315	0.0801
8	-0.0510	-0.5878	0.4310	-2.5970	0.2821	5.2322	0.0803
9	-0.0535	-0.6126	0.4370	-2.6897	0.2821	5.2327	0.0805
10	-0.0557	-0.6347	0.4424	-2.7729	0.2821	5.2330	0.0806
11	-0.0576	-0.6547	0.4473	-2.8483	0.2821	5.2333	0.0807

Table 3 Global deformation responses of the sandwich plates subjected to bending moment $M = 1$ Nmm ($h = 1$ mm, $h_c = 0.4h$, $2b = 3h$)

	[$\theta/-\theta/\text{core}/-\theta/\theta$]			[$\theta/-\theta/\text{core}/\theta/\theta$]			[$\theta/\theta/\text{core}/-\theta/-\theta$]		
	$C_6 \times 10^6$	$C_5 \times 10^6$	$C_3 \times 10^6$	$C_6 \times 10^6$	$C_5 \times 10^6$	$C_3 \times 10^6$	$C_6 \times 10^6$	$C_5 \times 10^6$	$C_3 \times 10^6$
0°	8.007×10^{-9}	30.9208	0	8.007×10^{-9}	30.9208	0	8.0076×10^{-9}	30.9208	0
15°	-3.763×10^{-7}	44.3292	26.5717	-3.620×10^{-7}	41.1557	1.839×10^{-6}	2.554×10^{-6}	76.9926	-2.110×10^{-5}
30°	3.848×10^{-7}	106.4730	29.9941	-7.442×10^{-7}	100.5105	-1.047×10^{-5}	4.594×10^{-6}	191.8378	-4.271×10^{-5}
45°	1.020×10^{-5}	273.8634	25.3157	9.299×10^{-6}	269.3253	3.624×10^{-7}	-5.158×10^{-5}	339.1102	-1.861×10^{-5}
60°	-3.765×10^{-6}	431.6471	12.7281	-6.781×10^{-6}	430.6543	1.199×10^{-5}	-6.750×10^{-6}	444.8586	-4.720×10^{-5}
75°	1.322×10^{-4}	482.2884	4.5749	1.340×10^{-4}	482.2090	-2.686×10^{-5}	-1.966×10^{-4}	482.9006	1.319×10^{-4}
90°	-4.722×10^{-5}	489.0269	0	-4.723×10^{-5}	489.0269	0	-4.723×10^{-5}	489.0269	0

sequence of the layers is written from the bottom surface to the top of the plate. For the plate that is subjected to bending moment, the dimensionless stress is defined as $\sigma^* = 2bh^2\sigma/M$. Each physical layer in the face is divided into p numerical layers and core is divided into $2p$ numerical layers and so the plate is divided into $N = 6p$ numerical layers. In this sandwich plate, $z = 0.5h_c$ indicates the core-face interface and $z = 0.5(h_f + h_c)$ shows the $-30^\circ/30^\circ$ interface at the top face. Table 3 shows the convergence of stresses by increasing the number of numerical layers. It is observed in Table 3 that at the free edge of plate in core-face interface ($z = 0.5h_c$, $y = b$) and in $-30^\circ/30^\circ$ interface ($z = 0.5(h_c + h_f)$, $y = b$), the out-of plane stresses σ_z and σ_{xz} do not converge and increase by increasing the number of numerical layers in the LW solution. At the point ($z = 0$, $y = b$) which is not the interface of physical layers, σ_{xz} converged for $p > 6$ to $\sigma_{xz} = 0.2821$. Also as seen in Table 2, the in-plane stresses σ_y and σ_x converge by increasing the number of numerical layers. It can be concluded that for obtaining accurate results in the LWT, the number of numerical layers in each physical layer of the laminate must be $p \geq 8$. In this study in order to obtain accurate results p is taken as 11.

3.3 Plate subjected to bending moment

The sandwich plate which is subjected to pure bending moment is studied in this section and the global response deformation of plate i.e., C_3 , C_5 and C_6 and also the in-plane and out of plane stresses are studied.

3.3.1 Global response of the plate

As noted before, C_6 , C_5 and C_3 which are clearly seen in Eq. (10) show the global deformation of the plate due to the loading. Table 3 shows the global deformation of sandwich plate with symmetric [$\theta/-\theta/\text{core}/-\theta/\theta$] and asymmetric [$\theta/-\theta/\text{core}/\theta/\theta$] and [$\theta/\theta/\text{core}/-\theta/-\theta$] layer stacking which is subjected to bending moment as $M = 1$ Nmm for various fiber orientations θ . The effect of the lamination sequence and fiber orientation on the global deformation response of the plate is obviously seen in this Table.

It is seen that bending moment M_x causes twisting in symmetric plate and extension in asymmetric plates. It must be noted that the global response of the plate to the bending moment can be interpreted by the A , B , and D matrix which are defined in the classical and first order shear deformation

theory (FSDT) of plates. It should be noted that in the FSDT, the extension-bending matrix B vanishes for the symmetric laminations such as [$\theta/-\theta/\text{core}/-\theta/\theta$], and so there is no bending-extension coupling in symmetric plates. Therefore as it is expected, in the prediction of LWT in Table 3, C_6 vanishes in pure bending of symmetric plate. For symmetric [$\theta/-\theta/\text{core}/-\theta/\theta$] plate, the term D_{16} and D_{26} which is bending-twisting coupling in the FSDT do not vanish, and so there is bending-twisting coupling for [$\theta/-\theta/\text{core}/-\theta/\theta$] plate, and as seen in Table 3, C_3 is not vanished in bending of [$\theta/-\theta/\text{core}/-\theta/\theta$] plate in the prediction of LWT. For [$\theta/-\theta/\text{core}/\theta/\theta$] and [$\theta/\theta/\text{core}/-\theta/-\theta$] plates, $B_{11} = B_{22} = B_{12} = D_{16} = D_{26} = 0$, so extension-bending and bending-twisting coupling are vanished for this laminations and as seen in Table 3, both C_6 and C_3 are vanished in pure bending of these plates.

3.3.2 Stress distribution

The distribution of out-of plane and in-plane stresses in the sandwich plate due to applied bending moment is studied. The [$30^\circ/-30^\circ/\text{core}/-30^\circ/30^\circ$] plate with $h_c = 0.4h$ and $h_f = 0.15h$ and $2b = 3h$ is studied and the dimensionless stress is defined as $\sigma^* = 2bh^2\sigma/M$.

The out of plane stresses arise near the edges because of mismatch in the mechanical properties of the layers. So the figures are focused on presentation of the distribution of out of plane normal and shear stresses along the interface and also through the thickness distribution of the stresses in the vicinity of the edges.

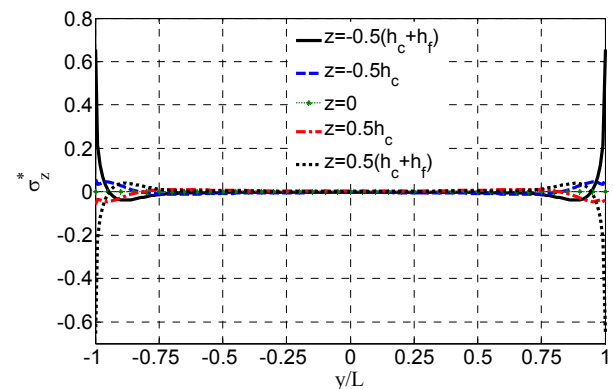


Fig. 7 Distribution of σ_z along the interfaces at [$30^\circ/-30^\circ/\text{core}/-30^\circ/30^\circ$] plate subjected to bending moment M

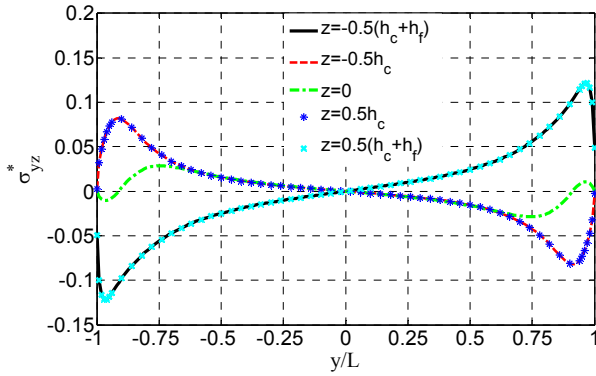


Fig. 8 Distribution of σ_{yz} along the interfaces at $[30^\circ/-30^\circ/\text{core}/-30^\circ/30^\circ]$ plate subjected to bending moment M

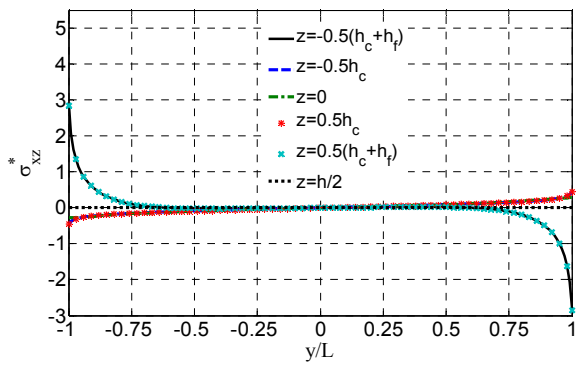


Fig. 9 Distribution of σ_{xz} along the interfaces at $[30^\circ/-30^\circ/\text{core}/-30^\circ/30^\circ]$ plate subjected to bending moment M

The distributions of out-of plane stresses along the width of the plate at $z = \pm 0.5h_c$, $z = \pm 0.5(h_c + h_p)$ and at the mid plane of the plate ($z = 0$) are shown in Figs. 7 to 9. The out of plane normal stress σ_z along the interfaces is shown in Fig. 7. As seen in the figure, σ_z vanishes far from the edges, and arises near the edges and the maximum of σ_z occurs at the interface of $30^\circ/-30^\circ$ layers exactly at the free edge. Due to the symmetry of the lamination in this plate, as Fig. 7 indicates, σ_z vanishes at mid plane of the plate and asymmetric distribution through the thickness of the plate is seen for σ_z .

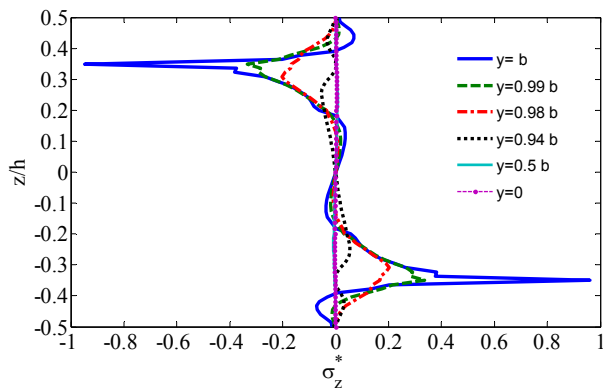


Fig. 10 Distribution of the out of plane normal stress σ_z through the thickness of $[30^\circ/-30^\circ/\text{core}/-30^\circ/30^\circ]$ plate

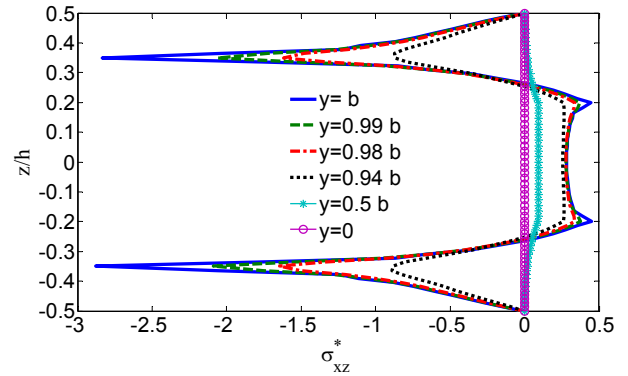


Fig. 11 Distribution of the out of plane shear stress σ_{xz} through the thickness of $[30^\circ/-30^\circ/\text{core}/-30^\circ/30^\circ]$ plate

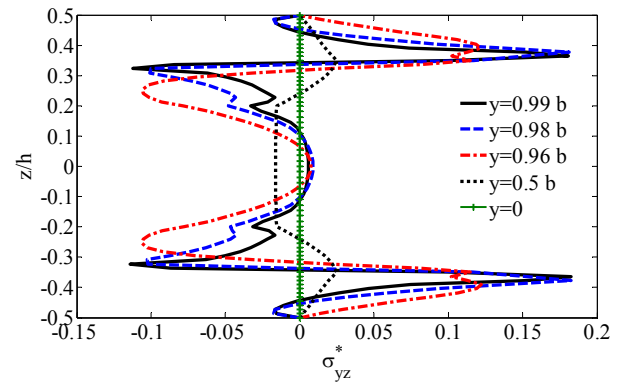


Fig. 12 Distribution of the out of plane shear stress σ_{yz} through the thickness of $[30^\circ/-30^\circ/\text{core}/-30^\circ/30^\circ]$ plate

The distributions of the out-of plane shear stresses σ_{yz} and σ_{xz} along the interface of the plate are shown in Figs. 8 and 9. As seen in Figs. 8 and 9, σ_{yz} gets its maximum in the vicinity of the free edges and σ_{xz} is maximum at the free edge $y = \pm b$ at the interface of the $-30^\circ/30^\circ$ layers. The normal stress σ_z has symmetric distribution and shear stress σ_{xz} and σ_{yz} have asymmetric distributions with respect to $y = 0$.

The distributions of the out of plane and in-plane stresses through the thickness of the plate in different sections at $y = b$, $0.99b$, $0.98b$, $0.94b$, $0.5b$ and $y = 0$ are shown in Figs. 10 to 14. The distributions of σ_z , σ_{xz} and σ_{yz} are presented in Figs. 10 to 12, respectively. Because of sharp mismatch in the mechanical properties of 30° and -30° layers, the out of plane stresses increased rapidly near the $30^\circ/-30^\circ$ interface. The maximum of σ_z and σ_{xz} are seen at the free edge at $-30^\circ/30^\circ$ interfaces. The stresses decreased by increasing the distance to the free edge. σ_z has asymmetric distribution and σ_{yz} and σ_{xz} have symmetric distribution through the thickness of plate. σ_{yz} has a sharp variation at $-30^\circ/30^\circ$ interfaces from the positive value to negative.

The distribution of the in-plane shear stress σ_{xy} and in-plane normal stress σ_y through the thickness of the sandwich plate is shown in Figs. 13 and 14. In-plane stresses σ_{xy} and σ_y have asymmetric distribution through the thickness of the plate. These stresses vanish at the free edge $y = b$, except in

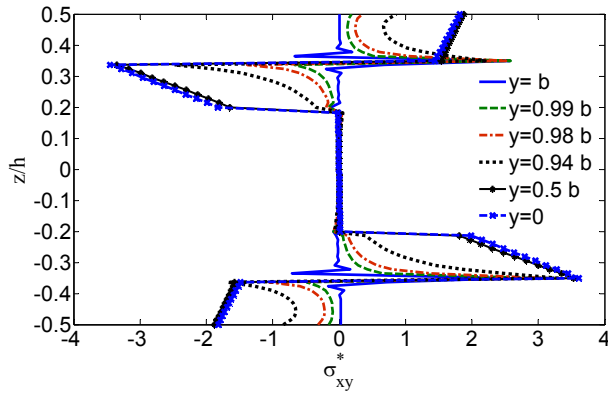


Fig. 13 Distribution of the in-plane shear stress σ_{xy} through the thickness of $[30^\circ/-30^\circ/\text{core}/-30^\circ/30^\circ]$ plate

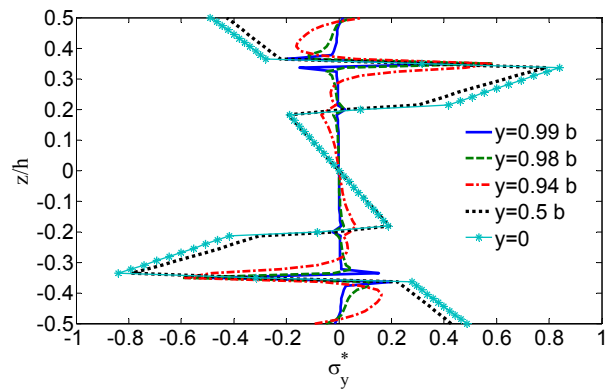


Fig. 14 Distribution of the in-plane normal stress σ_y through the thickness of $[30^\circ/-30^\circ/\text{core}/-30^\circ/30^\circ]$ plate

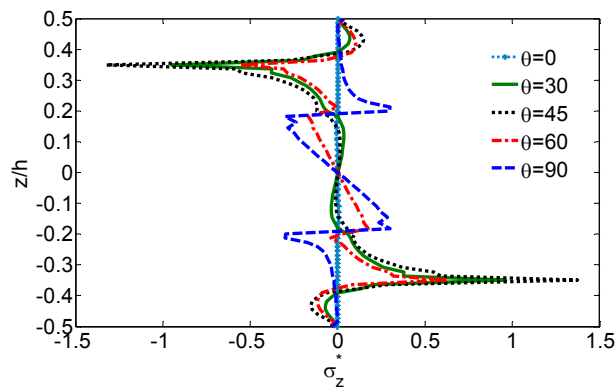


Fig. 15 Effect of fiber direction, θ on the distribution of σ_z at the free edge of $[\theta/-\theta/\text{core}/-\theta/\theta]$ plate

the $-30^\circ/30^\circ$ interfaces which the stresses do not converge at this point.

The amount of out of plane stresses depends on the mismatch between the mechanical properties of layers. So, the out of plane stresses depend on the orientation of fibers in the adjacent layers. The effect of fiber orientation θ in the $[\theta/-\theta/\text{core}/-\theta/\theta]$ plate on the distribution of σ_z and σ_{xz} at the free edge $y = b$ is presented in Figs. 15 and 16. It is

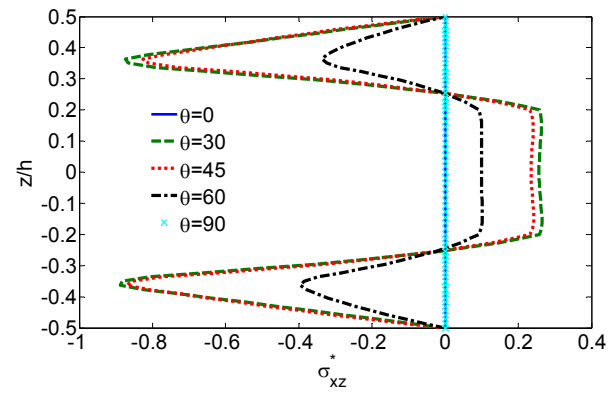


Fig. 16 Effect of fiber direction, θ on the distribution of σ_{xz} at the free edge of $[\theta/-\theta/\text{core}/-\theta/\theta]$ plate

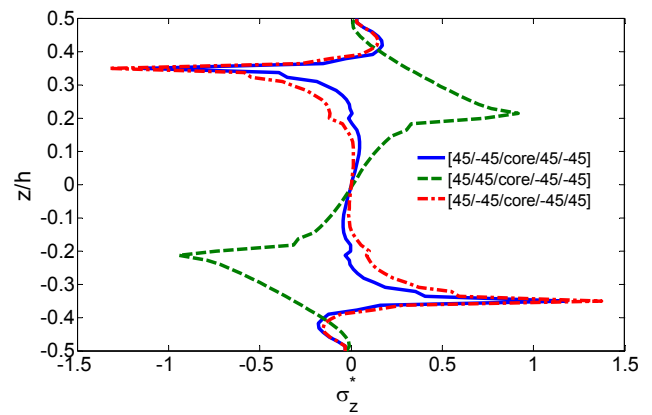


Fig. 17 Through the thickness distribution of σ_z at the free edge, $y = b$, of the plate for various layers stacking

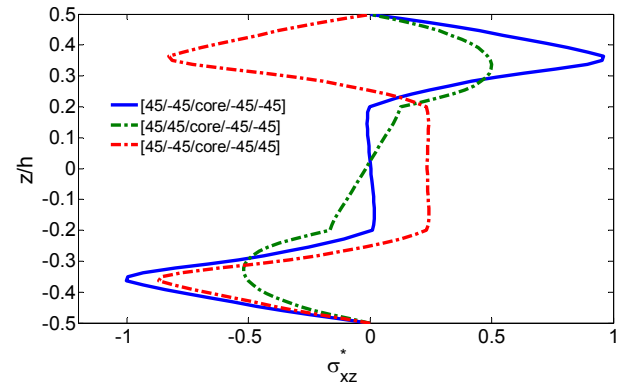


Fig. 18 Through the thickness distribution of σ_{xz} at free edge, $y = b$, of the plate for various layers stacking

observed in these Figures that in this plate σ_z is maximum for $\theta = 45^\circ$ and σ_{xz} is maximum for $\theta = 30^\circ$.

In order to study the effect of lamination sequence on the distribution of σ_z and σ_{xz} at the free edge, the distribution of stresses through the thickness of plate at $y = b$ in the plates with symmetric and un-symmetric lamination as $[45^\circ/-45^\circ/\text{core}/-45^\circ/45^\circ]$, $[45^\circ/45^\circ/\text{core}/-45^\circ/-45^\circ]$ and $[45^\circ/-45^\circ/\text{core}/45^\circ/-45^\circ]$ is depicted in Figs. 17 and 18. As seen in this figures, the lamination sequence effected the distribution of the out of plane stresses.

4. Conclusions

A layerwise formulation based on the Galerkin method is presented for discretization of the governing equations of long sandwich plate which is subjected to tension force and pure bending moment. The out of plane and in-plane stresses in the sandwich plate with laminated faces are studied. The appropriate displacement field is considered for the plate which includes the global response and local response of the plate and the governing equations are obtained based on the displacement components. An analytical method is used to solve the governing equations of the plate. The 3D stress state especially the out of plane stresses in the vicinity of the free edges of sandwich plate subjected to extension and pure bending is obtained. A 3D finite element model is used for verification of the accuracy of the predictions of present LW solution. The numerical results are presented and discussed for distribution of the out of plane and in-plane stresses in the plate due to bending moment and extension force. The effects of fiber direction and layer stacking on the global and local response and stress distribution of the sandwich plate are studied.

References

- Ahmadi, I. (2016), "Edge stresses analysis in thick composite panels subjected to axial loading using layerwise formulation", *Struct. Eng. Mech., Int. J.*, **57**(4), 733-762.
- Ahmadi, I. and Najafi, M. (2016), "Three-dimensional stresses analysis in rotating thin laminated composite cylindrical shells", *Steel Compos. Struct., Int. J.*, **22**(5), 1193-1214.
- Barbero, E.J. (2013), *Finite Element Analysis of Composite Materials using Abaqus*, CRC Press, Boca Raton, CA, USA.
- Basar, Y. and Ding, Y. (1995), "Interlaminar stress analysis of composites: Layerwise shell finite elements including transverse strains", *Compos. Eng.*, **5**(5), 485-499.
- Başar, Y., Itskov, M. and Eckstein, A. (2000), "Composite laminates: Nonlinear interlaminar stress analysis by multi-layer shell elements", *Comput. Methods Appl. Mech. Eng.*, **185**(2), 367-397.
- Cetkovic, M. and Vuksanovic, D. (2011), "Large deflection analysis of laminated composite plates using layerwise displacement model", *Struct. Eng. Mech., Int. J.*, **40**(2), 257-277.
- Cho, M. and Kim, H.S. (2000), "Iterative free-edge stress analysis of composite laminates under extension, bending, twisting and thermal loadings", *Int. J. Solids Struct.*, **37**(3), 435-459.
- Hamidi, A., Ahmed Houari, M.S., Mahmoud, S.R. and Tounsi, A. (2015), "A sinusoidal plate theory with 5-unknowns and stretching effect for thermomechanical bending of functionally graded sandwich plates", *Steel Compos. Struct., Int. J.*, **18**(1), 235-253.
- Hosseini Kordkheili, S.A. and Naghdabadi, R. (2005), "A finite element formulation for analysis of functionally graded plates and shells", *Arch. Appl. Mech.*, **74**(5), 375-386.
- Huang, B. and Kim, H.S. (2014), "Free-edge interlaminar stress analysis of piezo-bonded composite laminates under symmetric electric excitation", *Int. J. Solids Struct.*, **51**(6), 1246-1252.
- Huang, Y., Di, S., Wu, C. and Sun, H. (2002), "Bending analysis of composite laminated plates using a partially hybrid stress element with interlaminar continuity", *Comput. Struct.*, **80**(5), 403-410.
- Jin, N.W. (2008), "Damage analysis of laminated composite beams under bending loads using the layer-wise theory", Dissertation Thesis; Texas A&M University, TX, USA.
- Kim, T. and Atluri, S.N. (1994), "Interlaminar stresses in composite laminates under out-of-plane shear/bending", *AIAA J.*, **32**(8), 1700-1708.
- Kim, H., Lee, J. and Cho, M. (2012), "Free-edge interlaminar stress analysis of composite laminates using interface modeling", *J. Eng. Mech.*, **138**(8), 973-983.
- Kim, J.-S., Han, J.W. and Cho, M. (2016), "Boundary layer state prediction of composite and sandwich plates via an enhanced higher-order shear deformation theory", *Compos. Struct.*, **153**, 928-937.
- Lee, C.Y. and Chen, J.M. (1996), "Interlaminar shear stress analysis of composite laminate with layer reduction technique", *Int. J. Numer. Methods Eng.*, **39**(5), 847-865.
- Lekhnitskii, S.G. (1981), *Theory of Elasticity of an Anisotropic Body*, Mir Publisher, Moscow, Russia, 104 p.
- Lu, X. and Liu, D. (1990), "An interlaminar shear stress continuity theory" *Proceedings of the 5th Technical Conference of the American Society for Composites*, Lancaster, PA, USA, June, pp. 479-483.
- Matsunaga, H. (2002), "Assessment of a global higher-order deformation theory for laminated composite and sandwich plates", *Compos. Struct.*, **56**(3), 279-291.
- Matsunaga, H. (2004), "A comparison between 2-D single-layer and 3-D layerwise theories for computing interlaminar stresses of laminated composite and sandwich plates subjected to thermal loadings", *Compos. Struct.*, **64**(2), 161-177.
- Mittelstedt, C. and Becker, W. (2008), "Reddy's layerwise laminate plate theory for the computation of elastic fields in the vicinity of straight free laminate edges", *Mater. Sci. Eng.*, **498**(1), 76-80.
- Murthy, P.L.N. and Chamis, C.C. (1989), "Free-edge delamination: Laminate width and loading conditions effects", *J. Compos. Technol. Res.*, **11**(1), 15-22.
- Murugesan, N. and Rajamohan, V. (2015), "Investigation on interlaminar shear stresses in laminated composite beam under thermal and mechanical loading", *Steel Compos. Struct., Int. J.*, **18**(3), 583-601.
- Nosier, A. and Bahrami, A. (2007), "Interlaminar stresses in antisymmetric angle-ply laminates", *Compos. Struct.*, **78**(1), 18-33.
- Pipes, R.B. and Pagano, N.J. (1970), "Interlaminar stresses in composite laminates under uniform axial extension", *J. Compos. Mater.*, **4**(4), 538-548.
- Reddy, J.N. and Hsu, Y.S. (1980), "Effects of shear deformation and anisotropy on the thermal bending of layered composite plates", *J. Thermal Stress.*, **3**(4), 475-493.
- Robbins, D.H. and Reddy, J.N. (1993), "Modelling of thick composites using a layerwise laminate theory", *Int. J. Numer. Methods Eng.*, **36**(4), 655-677.
- Robbins, D.H. and Reddy, J.N. (1996), "Variable kinematic modelling of laminated composite plates", *Int. J. Numer. Methods Eng.*, **39**(13), 2283-2317.
- Rohwer, K. (1992), "Application of higher order theories to the bending analysis of layered composite plates", *Int. J. Solids Struct.*, **29**(1), 105-119.
- Rohwer, K., Rolfes, R. and Sparr, H. (2001), "Higher-order theories for thermal stresses in layered plates", *Int. J. Solids Struct.*, **38**(21), 3673-3687.
- Shu, X.P. and Soldatos, K.P. (2000), "Cylindrical bending of angle-ply laminates subjected to different sets of edge boundary conditions", *Int. J. Solids Struct.*, **37**(31), 4285-4307.
- Stein, M. (1986), "Nonlinear theory for plates and shells including the effects of transverse shearing", *AIAA J.*, **24**(9), 1537-1544.
- Tahani, M. and Andakhshideh, A. (2012), "Interlaminar stresses in thick rectangular laminated plates with arbitrary laminations

- and boundary conditions under transverse loads”, *Compos. Struct.*, **94**(5), 1793-1804.
- Tahani, M. and Nosier, A. (2003), “Edge effects of uniformly loaded cross-ply composite laminates”, *Mater. Des.*, **24**(8), 647-658.
- Wang, A.S.D. and Crossman, F.W. (1977), “Edge effects on thermally induced stresses in composite laminates”, *J. Compos. Mater.*, **11**(3), 300-312.
- Wu, C.P. and Kuo, H.C. (1992), “Interlaminar stresses analysis for laminated composite plates based on a local high order lamination theory”, *Compos. Struct.*, **20**(4), 237-247.
- Xiaohui, R., Wanji, C. and Zhen, W. (2011), “A new zig-zag theory and C^0 plate bending element for composite and sandwich plates”, *Arch. Appl. Mech.*, **81**(2), 185-197.
- Yasin, M.Y. and Kapuria, S. (2013), “An efficient layerwise finite element for shallow composite and sandwich shells”, *Compos. Struct.*, **98**, 202-214.
- Yin, W.L. (1994), “Simple solution of the free-edge stresses in composite laminates under thermal and mechanical loads”, *J. Compos. Mater.*, **28**(6), 573-586.
- Zhu, S.Q., Chen, X. and Wang, X. (2007), “Response of dynamic interlaminar stresses in laminated plates under free vibration and thermal load”, *Struct. Eng. Mech.*, **25**(6), 753-765.

CC

Appendix A

The stiffness matrix of each ply of the laminate which is used in Eq. (14) is considered as orthotropic material and can be written as

$$[\bar{C}] = \begin{bmatrix} \bar{C}_{11} & \bar{C}_{12} & \bar{C}_{13} & 0 & 0 & \bar{C}_{16} \\ \bar{C}_{12} & \bar{C}_{22} & \bar{C}_{23} & 0 & 0 & \bar{C}_{26} \\ \bar{C}_{13} & \bar{C}_{23} & \bar{C}_{33} & 0 & 0 & \bar{C}_{36} \\ 0 & 0 & 0 & \bar{C}_{44} & \bar{C}_{45} & 0 \\ 0 & 0 & 0 & \bar{C}_{45} & \bar{C}_{55} & 0 \\ \bar{C}_{16} & \bar{C}_{26} & \bar{C}_{36} & 0 & 0 & \bar{C}_{66} \end{bmatrix} \quad (A)$$

$[A_{pq}]$, $[B_{pq}]$, and $[D_{pq}]$ which are defined in Eq. (17) are $(N+1) \times (N+1)$ matrices and can be obtained as

$$(A_{pq}^{kj}, B_{pq}^{kj}) = \begin{cases} -\frac{\bar{C}_{pq}^{(k-1)}}{h_{k-1}}, -\frac{\bar{C}_{pq}^{(k-1)}}{2}, & \text{if } j = k-1 \\ \frac{\bar{C}_{pq}^{(k-1)}}{h_{k-1}} + \frac{\bar{C}_{pq}^{(k)}}{h_k}, \frac{\bar{C}_{pq}^{(k-1)}}{2} - \frac{\bar{C}_{pq}^{(k)}}{2}, & \text{if } j = k \\ -\frac{\bar{C}_{pq}^{(k)}}{h_k}, \frac{\bar{C}_{pq}^{(k)}}{2}, & \text{if } j = k+1 \\ (0, 0) & \text{if } j < k-1 \text{ or } j > k+1 \end{cases} \quad (A2)$$

$$D_{pq}^{kj} = \begin{cases} h_{k-1} \frac{\bar{C}_{pq}^{(k-1)}}{6} & \text{if } j = k-1 \\ h_{k-1} \frac{\bar{C}_{pq}^{(k-1)}}{3} + h_k \frac{\bar{C}_{pq}^{(k)}}{3}, & \text{if } j = k \\ h_{k-1} \frac{\bar{C}_{pq}^{(k)}}{6} & \text{if } j = k+1 \\ 0 & \text{if } j < k-1 \text{ or } j > k+1 \end{cases}$$

$\{A_{pq}\}$, $\{\tilde{A}_{pq}\}$, $\{B_{pq}\}$ and $\{\tilde{B}_{pq}\}$ are $(N+1) \times 1$ matrix and can be obtained as

$$A_{pq}^k = \begin{cases} -\bar{C}_{pq}^{(1)}, & \text{if } k = 1 \\ \bar{C}_{pq}^{(k-1)} - \bar{C}_{pq}^{(k)}, & \text{if } 1 < k < N+1 \\ \bar{C}_{pq}^{(N)}, & \text{if } k = N+1 \end{cases} \quad (A3)$$

$$\tilde{A}_{pq}^k = \begin{cases} -\bar{C}_{pq}^{(1)} \left(\frac{z_2 + z_1}{2} \right), & \text{if } k = 1 \\ \bar{C}_{pq}^{(k-1)} \left(\frac{z_k + z_{k-1}}{2} \right) - \bar{C}_{pq}^{(k)} \left(\frac{z_{k+1} + z_k}{2} \right), & \text{if } 1 < k < N+1 \\ \bar{C}_{pq}^{(N)} \left(\frac{z_{N+1} + z_N}{2} \right), & \text{if } k = N+1 \end{cases}$$

$$B_{pq}^k = \begin{cases} t_1 \frac{\bar{C}_{pq}^{(1)}}{2}, & \text{if } k = 1 \\ t_{k-1} \frac{\bar{C}_{pq}^{(k-1)}}{2} + t_k \frac{\bar{C}_{pq}^{(k)}}{2}, & \text{if } 1 < k < N+1 \\ t_N \frac{\bar{C}_{pq}^{(N)}}{2}, & \text{if } k = N+1 \end{cases} \quad (A4)$$

$$\tilde{B}_{pq}^k = \begin{cases} \frac{\tilde{C}_{pq}^{(1)}}{t_1} \left(\frac{z_2(z_2^2 - z_1^2)}{2} - \frac{(z_2^3 - z_1^3)}{3} \right) & \text{if } k=1. \\ \frac{\tilde{C}_{pq}^{(k-1)}}{t_{k-1}} \left(\frac{-z_{k-1}(z_k^2 - z_{k-1}^2)}{2} + \frac{z_k^3 - z_{k-1}^3}{3} \right) + \\ \frac{\tilde{C}_{pq}^{(k)}}{t_k} \left(\frac{z_{k+1}(z_{k+1}^2 - z_k^2)}{2} - \frac{z_{k+1}^3 - z_k^3}{3} \right), & \text{if } 1 < k < N+1. \\ \frac{\tilde{C}_{pq}^{(N)}}{t_N} \left(\frac{-z_N(z_{N+1}^2 - z_N^2)}{2} + \frac{z_{N+1}^3 - z_N^3}{3} \right) & \text{if } k=N+1. \end{cases} \quad (\text{A5})$$

Appendix B

The matrix $[C]$ in Eq. (22) are defines as

$$[C] = [B]^{-1}[A] \quad (\text{B1})$$

in which $[B]$ and $[A]$ are defined as

$$[B] = \begin{bmatrix} [I] & [0] & [0] & [0] & [0] & [0] \\ [0] & [D_{66}] & [0] & [D_{26}] & [0] & [0] \\ [0] & [0] & [I] & [0] & [0] & [0] \\ [0] & [D_{26}] & [0] & [D_{22}] & [0] & [0] \\ [0] & [0] & [0] & [0] & [I] & [0] \\ [0] & [0] & [0] & [0] & [0] & [D_{44}] \end{bmatrix} \quad (\text{B2})$$

where $[0]$ and $[I]$ mean zero and unity $(N+1) \times (N+1)$ matrix, respectively, and

$$[A] = \begin{bmatrix} [0] & [I] & [0] & [0] & [0] & [0] \\ [A_{55}] & [0] & [A_{45}] & [0] & [0] & -[B_{36}] + [B_{45}]^T \\ [0] & [0] & [0] & [I] & [0] & [0] \\ [A_{45}] & [0] & [A_{44}] & [0] & [0] & -[B_{23}] + [B_{44}]^T \\ [0] & [0] & [0] & [0] & [0] & [I] \\ [0] & -[B_{45}] + [B_{36}]^T & [0] & -[B_{44}] + [B_{23}]^T & [A_{33}] & [0] \end{bmatrix} \quad (\text{B3})$$

Also the column matrices $\{F_{31}\}$, $\{F_{32}\}$, $\{F_5\}$, $\{F_6\}$ in Eq. (22) are defined as

$$\begin{aligned} \{F_{31}\} &= [B]^{-1} \{\bar{F}_{31}\}, \\ \{F_{32}\} &= [B]^{-1} \{\bar{F}_{32}\}, \\ \{F_5\} &= [B]^{-1} \{\bar{F}_5\} \\ \{F_6\} &= [B]^{-1} \{\bar{F}_6\} \end{aligned} \quad (\text{B4})$$

where

$$\begin{aligned} \{\bar{F}_{31}\} &= \{ \{0\}^T, \{0\}^T, \{0\}^T, \{0\}^T, \{0\}^T, -\{\tilde{A}_{36}\}^T - \{B_{45}\}^T \} \\ \{\bar{F}_{32}\} &= \{ \{0\}^T, \{0\}^T, \{0\}^T, \{0\}^T, \{0\}^T, -\{\tilde{A}_{36}\}^T - \{B_{45}\}^T \} \\ \{\bar{F}_{32}\} &= \{ \{0\}^T, \{A_{55}\}^T, \{0\}^T, \{A_{45}\}^T, \{0\}^T, \{0\}^T \} \\ \{\bar{F}_5\} &= \{ \{0\}^T, \{0\}^T, \{0\}^T, \{0\}^T, \{0\}^T, \{\tilde{A}_{13}\}^T \} \\ \{\bar{F}_6\} &= \{ \{0\}^T, \{0\}^T, \{0\}^T, \{0\}^T, \{0\}^T, \{A_{13}\}^T \} \end{aligned} \quad (\text{B5})$$

and $[B]$ is defined in Eq. (B2).